

Durham Research Online

Deposited in DRO:

26 April 2013

Version of attached file:

Accepted Version

Peer-review status of attached file:

Peer-reviewed

Citation for published item:

Javaux, C. and Hughes, I.G. and Lothead, G. and Millen, J. and Jones, M.P.A. (2010) 'Modulation-free pump-probe spectroscopy of strontium atoms.', *European physical journal D.*, 57 (2). pp. 151-154.

Further information on publisher's website:

<http://dx.doi.org/10.1140/epjd/e2010-00029-4>

Publisher's copyright statement:

The original publication is available at www.springerlink.com

Additional information:

Use policy

The full-text may be used and/or reproduced, and given to third parties in any format or medium, without prior permission or charge, for personal research or study, educational, or not-for-profit purposes provided that:

- a full bibliographic reference is made to the original source
- a [link](#) is made to the metadata record in DRO
- the full-text is not changed in any way

The full-text must not be sold in any format or medium without the formal permission of the copyright holders.

Please consult the [full DRO policy](#) for further details.

Modulation-free pump-probe spectroscopy of strontium atoms

C. Javaux, I.G Hughes, G. Lochead, J. Millen, and M.P.A. Jones

Department of Physics, Durham University, Rochester Building, South Road, Durham DH1 3LE, United Kingdom, e-mail:
graham.lochead@durham.ac.uk

Received: date / Revised version: date

Abstract. We have performed polarization spectroscopy and sub-Doppler DAVLL on the $5s^2\ ^1S_0 \rightarrow 5s5p\ ^1P_1$ transition of atomic strontium. Both techniques generated a dispersion-type lineshape suitable for laser stabilization, without the need for frequency modulation. In both cases the signal is generated primarily by saturation effects, rather than optical pumping. The dependence of the amplitude and gradient on intensity and magnetic field were also investigated.

PACS. 32.30.Jc Visible and ultraviolet spectra – 42.62.Fi Laser spectroscopy

1 Introduction

The stabilization, or “locking”, of a laser frequency to an atomic transition is an essential technique for experiments in laser cooling and precision metrology. The starting point for laser locking is a spectroscopic technique which produces a lineshape with a zero crossing at the atomic resonance, providing an “error signal” that can be used to correct for frequency deviations. Suitable lineshapes with sub-Doppler spectroscopic resolution can be produced by using frequency modulated laser light, as in FM spectroscopy [1] or modulation transfer spectroscopy [2,3]. However it is not always straightforward, or desirable, to use frequency modulated light. If the modulation

is generated by modulating the injection current of a diode laser, then it is present on all the laser beams used in the experiments, which can cause problems for some experiments. For other laser sources, or where residual frequency modulation cannot be tolerated, a costly external modulator must be used. To get around this, spectroscopic techniques that generate a suitable lineshape directly, without the need for frequency modulation, have been developed. One such technique is polarization spectroscopy, which is widely used for both atoms and molecules [4,5]. A circularly polarized pump beam induces a birefringence in the medium, which is interrogated using a counterpropagating, linearly polarized probe beam at the same frequency.

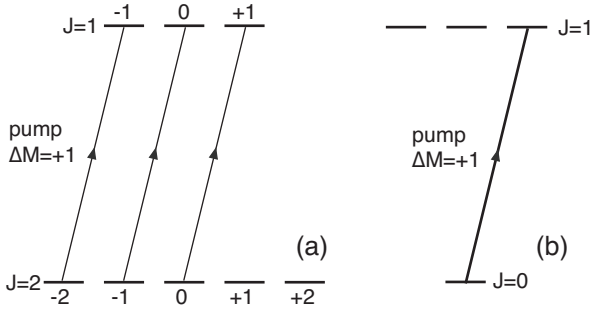


Fig. 1. (a) In conventional polarization spectroscopy, birefringence occurs because the degenerate m sublevels of the ground state are selectively depopulated by a circularly polarized pump beam. (b) Atoms such as Sr have a non-degenerate $J = 0$ ground state. Instead, the birefringence occurs because the strong circularly polarized pump beam leads to anisotropic saturation of the $5s^2\ ^1S_0 \rightarrow 5s5p\ ^1P_1$ transition.

In molecules, the birefringence is due to the selective depopulation of the degenerate magnetic sublevels of the ground state [5], as shown in figure 1a. In atoms with closed transitions such as the alkali metals Rb and Cs, optical pumping redistributes the population among the ground state sublevels and gives rise to the birefringent response [6, 7].

There is increasing interest in the spectroscopy and laser cooling of alkaline-earth elements and related atoms such as Yb, motivated by applications in precision frequency metrology [8] and ultra-cold Rydberg and plasma physics [9]. The situation here is very different. The naturally abundant bosonic isotopes have a single non-degenerate $J = 0$ ground state (figure 1b), which would seem to preclude the generation of a polarization spectroscopy signal.

In this paper, we explore two techniques for generating modulation-free signals for laser locking in atoms with a

$J = 0$ ground state, using the strong 461 nm $5s^2\ ^1S_0 \rightarrow 5s5p\ ^1P_1$ transition in strontium. We find that a polarization spectroscopy signal can be generated, which occurs due to the anisotropic saturation of the transition by the pump beam rather than optical pumping or selective depletion. This is a qualitatively different mechanism than previous work with the excited states of Ca, where optical pumping is important [10], and is responsible for the observation of polarization spectroscopy signals on the narrow Sr intercombination line at 689 nm in previous work [11]. To evaluate the performance of this polarization spectroscopy signal for laser locking, we compare it with the sub-Doppler DAVLL [12,13] technique, which also produces modulation-free signals. In this paper, both techniques are extensively characterized. In particular, the frequency stability of the zero-crossing point is evaluated by comparison to a conventional saturated absorption spectrum.

2 Polarization spectroscopy

The experimental arrangement for polarization spectroscopy is shown in figure 2. The output signal is the intensity difference between the two outputs of the polarizing beam-splitter cube. The probe beam is initially linearly polarized at $\phi = \pi/4$ to the axes of the cube such that the difference signal is zero in the absence of the pump beam. In the presence of the pump beam, the birefringence induced in the medium causes the probe beam polarization to be rotated through a small angle Φ , giving rise to a non-zero output signal. Expressions for the polarization

spectroscopy signal in this configuration were obtained in [6]. Neglecting the birefringence of the cell windows¹, the polarization spectroscopy signal after passing through a length L of the medium with absorption coefficient α is

$$I_{\text{signal}} = I_0 e^{-\alpha L} \cos(2\phi + 2\Phi(x)) , \quad (1)$$

with the rotation angle $\Phi(x)$ given by

$$\Phi(x) = L \frac{\Delta\alpha_0}{2} \frac{x}{1+x^2} , \quad (2)$$

where $\Delta\alpha_0$ is the on-resonance difference in absorption coefficient between the left- and right-hand circularly polarized components of the probe beam, and $x = 2(w-w_0)/\Gamma'$ is the detuning in units of half the power-broadened linewidth Γ' ².

The important parameter that sets the size of the polarization spectroscopy signal is the difference in line centre absorption $\Delta\alpha_0$ induced by the pump beam. In the alkali metals and molecules, this difference in absorption arises from an imbalance in the populations of the ground-state magnetic sublevels caused by the pump beam. This cannot occur in isotopes such as ^{88}Sr that have a $J = 0$ ground state and no nuclear spin, as these isotopes have a single non-degenerate ground state.

However a polarization spectroscopy signal can be generated on $J = 0 \rightarrow J = 1$ transitions such as the $5s^2\ ^1S_0 \rightarrow$

¹ Birefringence in the windows leads to a small additional rotation that can be compensated by adjusting slightly away from $\phi = \pi/4$. Variations can cause a slow drift of the laser lock point.

² The natural linewidth of the $5s^2\ ^1S_0 \rightarrow 5s5p\ ^1P_1$ transition is $\Gamma = 2\pi \times 32\text{ MHz}$.

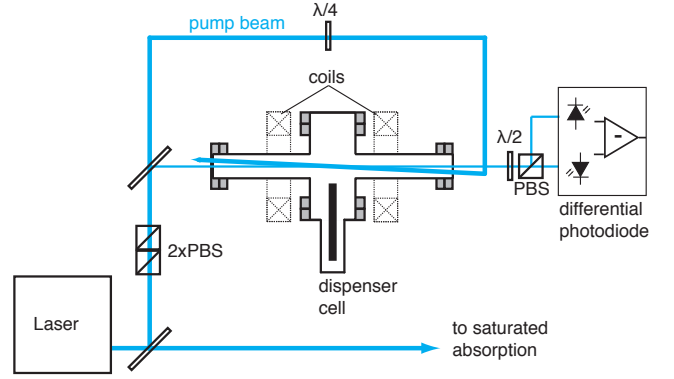


Fig. 2. (Colour online) Experimental layout for polarization spectroscopy. Polarizing beam splitter cubes (PBS) are used to set and analyse the polarization. For sub-Doppler DAVLL, the $\lambda/4$ plate is removed, the $\lambda/2$ plate is exchanged with a $\lambda/4$ plate and a magnetic field is applied along the axis using a pair of coils (shown dotted).

$5s5p\ ^1P_1$ transition in ^{88}Sr if the pump beam is strong enough. In this case the circularly polarized pump beam can saturate the σ_+ (or σ_-) components of the $J = 0 \rightarrow J = 1\ 5s^2\ ^1S_0 \rightarrow 5s5p\ ^1P_1$ transition, leading to reduced absorption of the corresponding component of the probe beam and a measurable birefringence. Even in the alkali metals, this mechanism can compete with optical pumping at high intensities, leading to a change in sign of the polarization spectroscopy signal [6,7].

Our experiment was set up as shown in figure 2. The 461 nm laser light was produced by a commercial frequency doubled diode laser system (Toptica-SHG). A novel dispenser-based vapour cell [14] was used for the measurements. A broad, weakly collimated jet of strontium atoms is produced by electrically heating a commercial vapour source. The pump and probe beams had $1/e^2$ radii of

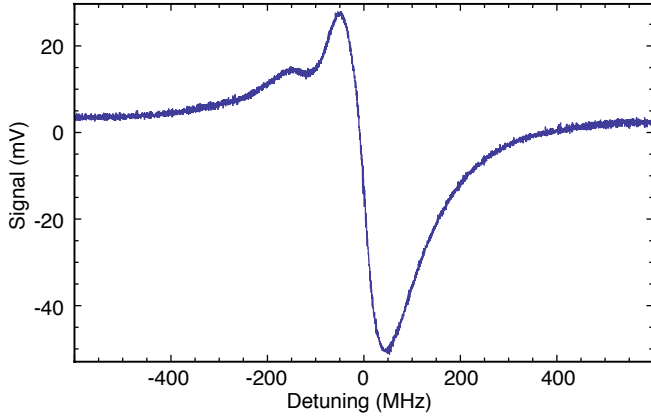


Fig. 3. The polarization spectroscopy signal, obtained with a pump beam intensity of 0.93 W cm^{-2} .

$0.67 \pm 0.05 \text{ mm}$ and $0.39 \pm 0.05 \text{ mm}$ in the horizontal and vertical directions respectively and were overlapped inside the cell with a small crossing angle ($\sim 20 \text{ mrad}$). The probe beam power was fixed at $41 \mu\text{W}$. An amplified differential photodiode was used to detect the light in the output arms of the PBS. A pair of coils placed symmetrically around the cell allowed a magnetic field to be applied along the direction of the laser beams. We also performed simultaneous saturated absorption spectroscopy using a second dispenser cell. The frequency axis of the laser scan was calibrated by fitting these saturated absorption spectra and using the known natural abundances, isotope shifts and hyperfine splittings [15].

An example of the polarization spectroscopy signal that we obtained is shown in figure 3. A sharp dispersion shaped feature associated with the dominant (83% abundant) ^{88}Sr isotope is clearly visible. This strong feature is ideal for laser locking. On the negative detuning side, contributions from the other isotopes are also visible. The peak signal is also lower on this side of resonance. The

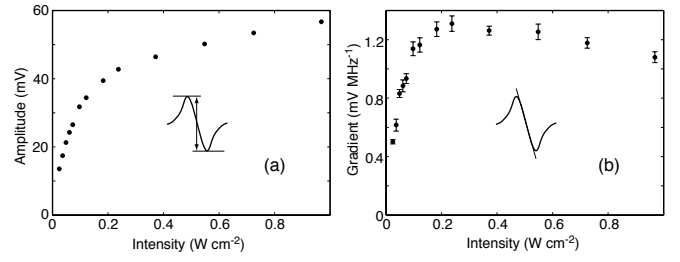


Fig. 4. Variation of the polarization spectroscopy signal amplitude (a) and gradient (b) with the pump beam intensity. Each point shows the mean value and standard error of five successive measurements. In (a) the size of this error bar is indicated by the size of the data points, and a 1.7% statistical error on the frequency axis calibration is included in the error bars for the gradient in (b). For the $5s^2\ ^1S_0 \rightarrow 5s5p\ ^1P_1$ transition, the theoretical saturation intensity is 0.043 W cm^{-2} .

shape of the signal here is very dependent on the pump and probe polarization, and is probably due to optical hyperfine pumping effects in the ^{87}Sr isotope.

By comparing the polarization spectroscopy signal with a saturated absorption spectrum acquired simultaneously in an atomic beam, we found that the zero-crossing is displaced from the centre of the ^{88}Sr resonance by approximately 10 MHz. This offset is important for laser locking, and it can be varied (and brought to zero) by making slight adjustments to the angle ϕ of the $\lambda/2$ plate. We have investigated the stability of this offset, and we find that the RMS variation of the offset during a ~ 1 hour period is 0.8 MHz. The variation of the amplitude and gradient of the polarization spectroscopy signal is shown in figure 4. At high pump intensity ($I \gg I_{\text{sat}}$), the amplitude saturates as expected, while the gradient reaches a maximum

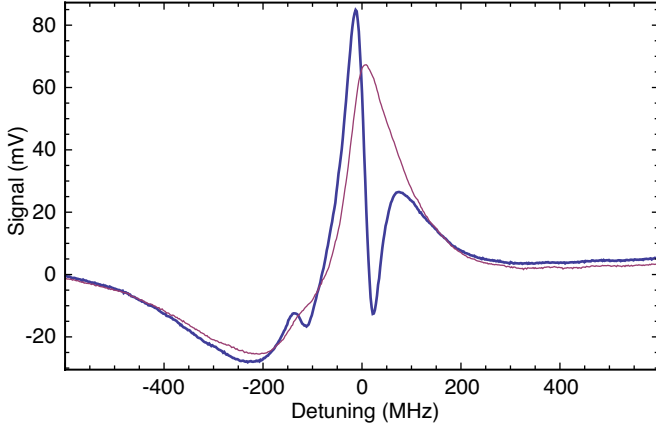


Fig. 5. (Colour online) An example sub-Doppler DAVLL signal (thick blue line), obtained with a pump beam intensity of 0.42 W cm^{-2} and a magnetic field of 8.5 G. A sharp sub-Doppler dispersion feature is superimposed on the Doppler-broadened background DAVLL signal (thin red line).

before decreasing again as power broadening becomes important.

A quantitative model of the polarization spectroscopy signal would have to take into account the spatial profile of the beam and the time-dependence of the anisotropy. For rubidium vapour in thermal equilibrium, the time-dependent anisotropy has recently been calculated analytically and numerically [16]. In our experiment, the velocity distribution of atoms in the jet from the dispenser source is not well characterized, and so a quantitative simulation is beyond the scope of this work. However, we can use (1) to estimate the rotation angle. From the peak signal at positive detuning, we estimate the maximum rotation angle Φ to be $\sim 2 \text{ mrad}$.

3 Sub-Doppler DAVLL

In order to obtain sub-Doppler DAVLL signals, the half-wave plate before the analyzer cube is replaced with a quarter-wave plate. The axes of this waveplate are adjusted to be at $\pi/4$ with respect to the initial linear polarization. In this configuration, the two circular components of the linearly polarized probe beam exit from different ports of the analyzer cube. Therefore the difference in intensity between the two outputs corresponds to the difference in absorption on the σ_+ and σ_- transitions (circular dichroism). A magnetic field applied along the axis of the probe beam lifts the degeneracy between the $m_J = 0, \pm 1$ sublevels of the $5s5p \text{ } ^1\text{P}_1$ excited state, Zeeman shifting the centres of the σ_+ and σ_- transitions equally but in opposite directions. Hence above or below the zero-field resonance one circular component is absorbed more than the other, while exactly on resonance the difference signal is zero. Conventional DAVLL [17,18] uses a probe beam only, and it is the Doppler-broadened absorption line that must be Zeeman split by the magnetic field. In sub-Doppler DAVLL, a linearly polarized pump beam is added (by removing the quarter-wave plate in figure 2), and sharp dispersion features are obtained at much lower magnetic fields by splitting the sub-Doppler spectral lines. In strontium, these sub-Doppler features originate solely from saturation, whereas in the alkali metals hyperfine pumping is the dominant mechanism [19].

An example of the sub-Doppler DAVLL signal that we obtained is shown in figure 5. Again, a sharp sub-Doppler feature with a zero-crossing close to the atomic resonance

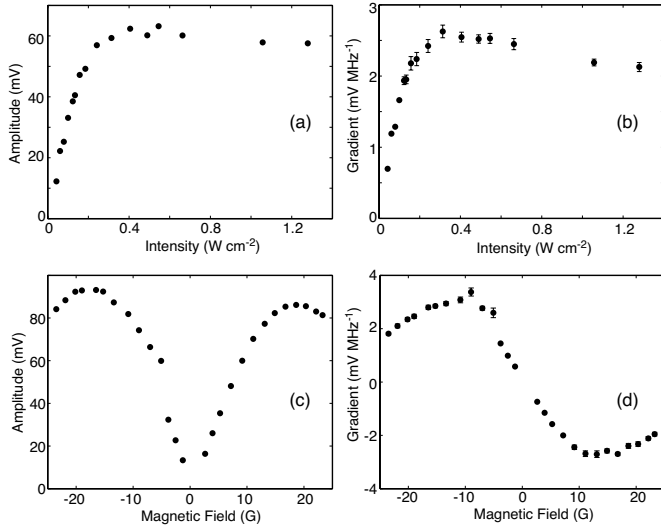


Fig. 6. (a and b) Variation of the amplitude (a) and gradient (b) of the sub-Doppler DAVLL signal as a function of intensity, with the magnetic field fixed at 9.5 G. (c and d) Variation of the amplitude (c) and gradient (d) of the sub-Doppler DAVLL signal with magnetic field. The pump intensity was fixed at 0.66 W cm^{-2} .

frequency is obtained. However, this steep sub-Doppler feature is superimposed on a background Doppler-broadened DAVLL signal, in contrast to the polarization spectroscopy where the Doppler-broadened background absorption is cancelled completely in the difference signal. The variation of the amplitude and gradient with magnetic field and pump beam intensity is shown in figure 6. The amplitude and gradient are comparable to that obtained from polarization spectroscopy with the same pump and probe power (figure 4), and follow the same trends. Both the amplitude and gradient depend strongly on the size of the applied magnetic field, increasing to a maximum as the field is increased before decreasing again at very high fields. The optimum gradient should occur when the differential Zeeman

shift between the σ_+ and σ_- transitions is equal to the power-broadened linewidth. Here, the maximum gradient is reached at approximately 12 G, which corresponds to a differential Zeeman shift of 34 MHz, indicating a small power-broadening of the line at this pump beam intensity. The maximum amplitude occurs at slightly higher magnetic field than the maximum gradient. We have also characterized the variation in the offset between the zero-crossing of the sub-Doppler DAVLL signal and the atomic line centre. This offset depends slightly on the applied magnetic field, varying between 10 and 30 MHz. At a fixed magnetic field, the offset is slightly less stable than for polarization spectroscopy, varying by less than 3 MHz over a similar 1 hour period.

4 Discussion and Conclusions

We have applied polarization spectroscopy and sub-Doppler strontium. Both techniques generate dispersion-shaped lines with sub-Doppler resolution that are suitable for laser locking. With this application in mind, it is instructive to compare the two techniques. For a given laser power, the two techniques produce signals with a similar amplitude and gradient. However, the sub-Doppler DAVLL signal is superimposed on a large Doppler-broadened background, whereas the polarization spectroscopy signal has no Doppler-broadened component. This flat background is responsible for the greater stability in the zero-crossing position that we observed for polarization spectroscopy. In our laboratory we use polarization spectroscopy to rou-

tinely stabilize our 461 nm laser for laser-cooling and Rydberg spectroscopy experiments.

This work was supported by EPSRC grants nos. EP/D070287/1 and EP/D502594/1, and the Royal Society.

References

1. G.C. Bjorklund, *Optics Letters* **5**, 15 (1980).
2. J.H. Shirley, *Optics Letters* **7**, 537 (1982).
3. D.J. McCarron, S.A. King, S.L. Cornish, *Meas. Sci. Technol.* **19**, 105601 (2008).
4. C. Wieman, T.W. Hänsch, *Phys. Rev. Lett.* **36**, 1170 (1976).
5. W. Demtroder, *Laser Spectroscopy: Basic Concepts and Instrumentation* (Springer-Verlag, 1996) 454–465
6. C.P. Pearman, C.S. Adams, S.G. Cox, P.F. Griffin, D.A. Smith, I.G. Hughes, *J. Phys. B: At. Mol. Opt. Phys.* **35**, 5141 (2002).
7. M.L. Harris, C.S. Adams, S.L. Cornish, I.C. McLeod, E. Tarleton, I.G. Hughes, *Phys. Rev. A* **73**, 062509 (2006).
8. S. Blatt, A.D. Ludlow, G.K. Campbell, J.W. Thomsen, T. Zelevinsky, M.M. Boyd, J. Ye, X. Baillard, M. Fouché, R. Le Targat, Brusch, P. Lemonde, M. Takamoto, F.L. Hong, H. Katori, V.C. Flambaum, *Phys. Rev. Lett.* **100**, 140801 (2008).
9. C.E. Simien, Y.C. Chen, P. Gupta, S. Laha, Y.N. Martinez, P.G. Mickelson, D.B. Nagel, T.C. Killian, *Phys. Rev. Lett.* **92**, 143001 (2004).
10. D. Hansen, A. Hemmerich, *Phys. Rev. A* **72**, 022502 (2005).
11. G.M. Tino, M. Barsanti, M. de Angelis, L. Gianfrani, M. Inguscio, *Appl. Phys. B* **55**, 397 (1992).
12. G. Wasik, W. Gawlik, J. Zachorowski, W. Zawadzki, *Appl. Phys. B* **75**, 613 (2002).
13. M.L. Harris, S.L. Cornish, A. Tripathi, I.G. Hughes, *J. Phys. B: At. Mol. Opt. Phys.* **41**, 085401 (2006).
14. E.M. Bridge, J. Millen, C.S. Adams, M.P.A. Jones, *Rev. Sci. Instr.* **80**, 013101 (2009).
15. S. Mauger, J. Millen, M.P.A. Jones, *J. Phys. B: At. Mol. Opt. Phys.* **40**, F319 (2007).
16. H. Do, G. Moon, H.-R. Noh, *Phys. Rev. A* **77**, 032513 (2008).
17. B. Chéron, H. Gilles, J. Hamel, O. Moreau, H. Sorel, *J. Phys. III* **4**, 401 (1994).
18. K.L. Corwin, Z.-T. Lu, C.F. Hand, R.J. Epstein, C.E. Wieman, *Appl. Opt.* **37**, 3295 (1998).
19. D.A. Smith, I.G. Hughes, *Am. J. Phys.* **72**, 631 (2004).